AD-756 183

THERMAL ANALYSIS OF PLATES WITH CIRCULAR INCLUSIONS

A. L. McFall, et al

Notre Dame University

Prepared for:

Office of Nava Research

February 1973

DISTRIBUTED BY:

NTIS

National Technical Information Service
U. S. DEPARTMENT OF COMMERCE
5285 Port Royal Road, Springfield Va. 22151

AD756183

THERMAL ANALYSIS OF PLATES WITH CIRCULAR INCLUSIONS

by

A. L. McFall, T. Ariman and L. H. N. Lee

February, 1973

DISTRIBUTION OF THIS DOCUMENT IS UNLIMITED

Deep Ocean Engineering

CONTRACT ONR-N00014-68-A-0152

University of Notre Dame
college of engineering
notre dame, indiana

D D C
RECEIVED
FEB 28 1973
E

Reproduced by
NATIONAL TECHNICAL
INFORMATION SERVICE
U S Department of Commerce
Springfield VA 22151

42

NUMBER:
UND-73-2

THERMAL ANALYSIS OF PLATES WITH CIRCULAR INCLUSIONS

by

A. L. McFall, T. Ariman and L. H. N. Lee

February, 1973

Document cleared for public release and sale:

Distribution is unlimited.

University of Notre Dame
College of Engineering
Notre Dame, Indiana 46556

Contract
N00014-68-A-0152(NR 260-112/7-13-67)
Office of Naval Research

TECHNICAL REPORT
NUMBER:
UND-73-2

I

UNCLASSIFIED

Security Classification

DOCUMENT CONTROL DATA - R&D

(Security classification of title, body of abstract and indexing annotation must be entered when the overall report is classified)

1 ORIGINATING ACTIVITY *(Corporate author)* College of Engineering University of Notre Dame Notre Dame, Indiana 46556	2a REPORT SECURITY CLASSIFICATION UNCLASSIFIED 2b GROUP

3 REPORT TITLE

THERMAL ANALYSIS OF PLATES WITH CIRCULAR INCLUSIONS

4 DESCRIPTIVE NOTES *(Type of report and inclusive dates)*

5 AUTHOR(S) *(Last name, first name, initial)*

McFall, A. L., Ariman, T., and Lee, L. H. N.

6. REPORT DATE January, 1973	7a. TOTAL NO. OF PAGES 35	7b. NO. OF REFS 25
8a. CONTRACT OR GRANT NO. ONR-N00014-68-A-0152 b. PROJECT NO. In-House Acct. No. 2400-24038 c d.	9a. ORIGINATOR'S REPORT NUMBER(S) UND-73-2 9b. OTHER REPORT NO(S) *(Any other numbers that may be assigned this report)*	

10 AVAILABILITY/LIMITATION NOTICES

Document cleared for public release and sale. Its distribution is unlimited.

11. SUPPLEMENTARY NOTES	12. SPONSORING MILITARY ACTIVITY Department of the Navy

13. ABSTRACT

A least square boundary point matching method is employed to determine the temperature distributions and deformations of rectangular plates with circular elastic inclusions. Solutions for two problems have been obtained. The first problem is concerned with the determination of the temperature distribution in a finite rectangular plate having a circular inclusion and subjected to prescribed temperature distribution and thermal conditions along the edges. The plate is heated uniformly through the thickness. The second problem is concerned with the deflection and moment distribution in the same plate model with simply supported edges and prescribed temperature variation across the thickness but no temperature variation over the plate surface. Numerical results are presented.

Ia

DD FORM 1473

UNCLASSIFIED

Security Classification

14 KEY WORDS	LINK A ROLE	LINK A WT	LINK B ROLE	LINK B WT	LINK C ROLE	LINK C WT
RECTANGULAR PLATE						
ELASTIC CIRCULAR INCLUSION						
TEMPERATURE DISTRIBUTION						
PLATE DEFLECTION						
BOUNDARY POINT MATCHING						

Ib

FOREWORD

This technical report was prepared by the Dynamical Systems Group under the Deep Sea Engineering Project at the University of Notre Dame, College of Engineering. The authors, A. L. McFall, T. Ariman, and L. H. N. Lee are, respectively, Graduate Research Assistant, Associate Professor and Professor in the Department of Aerospace and Mechanical Engineering.

The research was performed under the sponsorship of the Department of the Navy, Office of Naval Research, Washington, D.C. 20360, with funding under Contract N00014-68-A-0152 and In-House Account Number UND-2400-24038.

Readers are advised that reproduction in whole or in part is permitted for any purpose of the United States Government.

This technical report has been reviewed and approved for submittal to the sponsoring agency January, 1973

EDWARD W. JERGER
PROGRAM MANAGER

JOSEPH C. HOGAN
DEAN, COLLEGE OF ENGINEERING
UNIVERSITY OF NOTRE DAME

TABLE OF CONTENTS

	Page
INTRODUCTION	1
TEMPERATURE DISTRIBUTION	3
THERMAL BENDING	7
APPENDIX A	15
APPENDIX B	17
REFERENCES	19

Preceding page blank

LIST OF FIGURES

		page
Fig. 2.1	System of coordinates for temperature distribution.	21
Fig. 2.2	Typical boundary layout for "point-matching".	22
Fig. 2.3	Temperature function ω, plotted as a function of inclusion size and $\theta = .1$, $a/b = 1.0$, and $r = R$.	23
Fig. 2.4	Temperature function ω, plotted as a function of λ and θ for $R/b = .5$, $a/b = 1.0$, and $r = R$.	24
Fig. 2.5	Temperature function ω, plotted as a function of a/b and θ, with $R/b = .5$ and $\lambda = .1$, and $r = R$.	25
Fig. 2.6	Temperature function ω, plotted as a function of X and Y with $R/b = .5$, $a/b = 1.0$, $\lambda = 10$.	26
Fig. 2.7	Temperature function ω, plotted as a function of X and Y with $R/b = .5$, $a/b = 1.0$, $\lambda = .1$.	27
Fig. 2.8	Temperature function ω, plotted as a function of X and λ with $R/b = .75$, $a/b = 1.0$, $y = 0.0$.	28
Fig. 3.1	Simply supported rectangular plate with circular inclusion - coordinate system.	29
Fig. 3.2	Plate deflection as a function of R/b with $\eta = .1$, $\rho = 1.0$, and $\nu_a = \nu_b = .3$.	30
Fig. 3.3	Plate deflection as a function of R/b with $\eta = 10.0$, $\rho = 1.0$, and $\nu_a = \nu_b = .3$.	31
Fig. 3.4	Plate deflection as a function of θ with $\eta = 10$, $\rho = 1.0$, $R/b = .5$ and $\nu_a = \nu_b = .3$.	32
Fig. 3.5	Plate deflection as a function of θ with $\eta = .1$, $\rho = 1.0$, $R/b = .5$ and $\nu_a = \nu_b = .3$.	33
Fig. 3.6	Plate deflection as a function of η with $R/b = .5$, $\rho = 1.0$ and $\nu_a = \nu_b = .3$.	34
Fig. 3.7	Plate deflection as a function of ρ with $\eta = 1.0$, $R/b = .15$, $\nu_a = \nu_b = .3$.	35

I. INTRODUCTION

It is a common knowledge that plates are essential structural elements for constructing marine vehicles. To serve their functions, most plates may have holes and elastic inclusions and be subjected to temperature gradients. It is the objective of this research to develop an approach for the determination of temperature distributions, thermal stresses and deformation of rectangular plates with circular inclusions. It is assumed that both the plates and inclusions are individually homogeneous and isotropic.

In the last decade, several papers on membrane thermal stresses in infinite plates with holes appeared in the literature. Goodier and Florence published a number of articles [1-6] on localized thermal stress at holes, cavities and inclusions caused by disturbed uniform heat flow. It is well known that in an infinite plate a steady heat flow under a uniform temperature gradient does not induce thermal stress provided the plate is free to expand. Thermal stress is induced, however, if the uniform flow of heat is disturbed by the presence of an insulated circular hole, or by an inclusion of another material. The influence of the shape and rigidity of an elastic inclusion on the transverse flexure of thin plates was investigated by Goland [7]. Tauchert [8] analyzed thermal stresses at spherical inclusions in uniform heat flow. Recently Hoffman and Ariman [9], Rao, Rao and Ariman [10, 11] have used the least squares boundary point matching method to investigate the temperature, bending and membrane stress distributions for a rectangular elastic plate with circular [10] and elliptic [11] holes subject to heat flow.

On the other hand in many cases a satisfactory solution for a given boundary value problem can be obtained by the method of point matching. A simple description of this technique is that solutions are used which satisfy the governing differential equations exactly, while approximating the boundary conditions at discrete points on the boundary. This procedure proves very useful for problems in which no exact theoretical analysis can be formulated. Furthermore a single computer program can be used for any problem governed by that equation without regarding the shape of the boundary.

The concept of the least squares boundary point matching method (see Appendix A) occurred to several investigators as early as 1934, Slater [12] and 1937, Barta [13]. The method was not used extensively until 1960 when Conway [14], after recognizing the method's potential for a wide class of problems, named this technique "point-matching". Since then, the method has been developed particularly for the bending of plates by Leissa and Niedenfuhr [15] and has been applied to numerous other boundary value problems [16-19]. Eringen and his co-workers extended this method to stress concentration problems in shells with holes and to the problem of two normally intersecting circular cylindrical shells [20-22].

In the first problem of this study, the temperature distribution in a finite rectangular plate with a circular inclusion is investigated by the same method. The plate is heated uniformly through the thickness, that is the temperature varies only along the coordinates within the plane. Two opposite edges of the plate are kept at constant temperatures while the other edges are insulated.

In the second problem, the deflection and moment distribution in the same plate model with simply supported edges is investigated by the least squares point matching method. The heat flow consists of an arbitrary temperature variation across the thickness of the plate, but with no variation over the plate surface. For both problems the solutions are derived in the form of an infinite series in terms of circular cylindrical coordinates r and θ. The boundary conditions at the inclusion interface are satisfied exactly while the ones at the simply supported edges of the rectangular plate are satisfied at selected points by the least squares method. Numerical results are presented for temperature distribution, deflections and moments as a function of the ratio of elastic properties of the plate and inclusion, and the inclusion size.

II. TEMPERATURE DISTRIBUTION

A rectangular elastic thin plate of uniform thickness is subjected to heat flow in the x-direction (Fig. 2. 1.) The edges at $y = \pm b$, of the plate are insulated. The surfaces at $x = \pm a$ are held at constant temperatures T_1 and T_2 with $T_1 > T_2$. A circular cylindrical inclusion with different thermal properties than the plate is centrally located with the plate. The governing equation for the steady-state heat conduction in a thin plate with no sources or sinks is the Laplace equation [23].

$$\nabla^2 T = 0 \tag{2. 1}$$

where

$$\nabla^2 = \frac{\partial^2}{\partial r^2} + \frac{1}{r}\frac{\partial}{\partial r} + \frac{1}{r^2}\frac{\partial^2}{\partial \theta^2} \tag{2. 2}$$

and $T(r, \theta)$ is the temperature. The boundary conditions are given by

$$\begin{aligned} T &= T_1 \text{ at } x = a \\ T &= T_2 \text{ at } x = -a \end{aligned} \tag{2. 3}$$

$$\frac{\partial T}{\partial y} = 0 \text{ at } y = \pm b \tag{2.4}$$

$$T_a = T_b \text{ and } K_a \frac{\partial T_a}{\partial r} = K_b \frac{\partial T_b}{\partial r} \text{ at } r = R \tag{2.5}$$

Equations (2.3) and (2.4) are the boundary conditions at the edge of the plate, while equations (2.5) apply at the boundary of the circular inclusion and the plate. In these eqs. K_a and K_b represent thermal conductivity of the inclusion and plate materials respectively.

The general solution to Eq. (2.1) in plane polar coordinates can be represented as

$$T(r,\theta) = \frac{1}{2}(\alpha_o + \beta_o \ln r) + \sum_{n=1}^{\infty} [\alpha_n r^n + \beta_n r^{-n}) \cos n\theta + (\gamma_n r^n + \delta_n r^{-n}) \sin n\theta] \tag{2.6}$$

where α_n, β_n, γ_n and δ_n are unknown coefficients to be determined from the boundary conditions. By considering the symmetry of the problem about the x-axis, this solution reduces to:

For the plate: $T_b(r,\theta) = \frac{1}{2}(\alpha_{ob} + \beta_{ob} \ln r) + \sum_{n=1}^{\infty} [(\alpha_{nb} r^n + \beta_{nb} r^{-n}) \cos n\theta$ (2.7)

For the inclusion: $T_a(r,\theta) = \frac{1}{2}(\alpha_{oa} + \beta_{oa} \ln r) + \sum_{n=1}^{\infty} (\alpha_{na} r^n + \beta_{na} r^{-n}) \cos n\theta$ (2.8)

where T_b and T_a represent temperatures in the plate and in the inclusion respectively. T_a should remain finite as r approaches zero in the inclusion, therefore it is easily seen that $\beta_{oa} = \beta_{na} = 0$ and T_a takes the following form

$$T_a(r,\theta) = \frac{\alpha_{oa}}{2} + \sum_{n=1}^{\infty} (\alpha_{na} r^n) \cos n\theta \tag{2.9}$$

Eqs. (2.7) and (2.9) by the use of boundary conditions around the circular inclusion Eqs. (2.4) and (2.5), yield the following relationships:

$$\alpha_{ob} + \beta_{ob} \ln R = \alpha_{oa} \tag{2.10}$$

$$\alpha_{nb} R^{n} + \beta_{nb} R^{-n} = \alpha_{na} R^{n} \tag{2.11}$$

$$\beta_{ob} = 0 \tag{2.12}$$

$$K_b(\alpha_{nb} R^{n-1} - \beta_{nb} R^{-n-1}) = K_a (\alpha_{na} R^{n-1}) \tag{2.13}$$

From Eqs. (2.10) and (2.12)

$$\alpha_{ob} = \alpha_{oa} \tag{2.14}$$

anf from (2.11) and (2.13)

$$\beta_{nb} = \alpha_{nb} R^{2n} \frac{K_b - K_a}{K_a + K_b} \tag{2.15}$$

Substituting Eqs. (2.12), (2.14) and (2.15) into (2.7) and (2.9) one obtains

$$\text{for } r > R \quad T_b(r,\theta) = \frac{\alpha_{ob}}{2} + \sum_{n=1}^{\infty} \alpha_{nb}(r^{n} + R^{2n} \Psi r^{-n}) \cos n\theta \tag{2.16}$$

$$\text{for } r < R \quad T_a(r,\theta) = \frac{\alpha_{ob}}{2} + \sum_{n=1}^{\infty} \alpha_{nb}(1 + \Psi) r^{n} \cos n\theta \tag{2.17}$$

where

$$\Psi = \frac{K_b - K_a}{K_b + K_a} \tag{2.18}$$

For the case of an circular hole in the same plate $K_a = 0$, $\Psi = 1$ and Eq. (2.16) is in agreement with the one given by Rao et al [10].

The unknown coefficients α_{ob} and α_{nb} are now determined by satisfying the boundary conditions at the outer edges of the plate (Eqs. (2.3) and (2.4)). However, since the boundaries $x = \pm a$ and $y = \pm b$ are not coordinate lines for the temperature function, an exact solution cannot be found. To obtain an approximate solution the infinite series in Eqs. (2.16) and (2.17) is truncated at $n = N$ terms, leaving $n + 1$ coefficients to be determined. M points are chosen along the plate outer boundaries. As there is one condition for each point, M equations are generated. For $M = N + 1$, the

equations may be solved for the required coefficients. However, if $M > N + 1$ and the unknowns are determined in the least squares sense, then as $M \to \infty$ this process becomes that of minimizing the integral of the squared error.

In order to get some numerical values for the problem T_1 and T_2 are chosen as $150^{\circ}F$ and $100^{\circ}F$ respectively. The number of boundary points taken is forty (M=40) Fig. (2. 2) and eight terms (N=8) are considered in the series. Thus forty equations for nine unknowns are generated. Solving these in the least squares sense yields the necessary coefficients α_n.

In Fig. (2. 3), the variation of the nondimensionalized temperature function $\phi = \frac{T - T_2}{T_1 - T_2}$ is presented on the perimeter of the inclusion in a square plate. The curves are given for various sizes of the circular inclusion and no inclusion case with $R/b = 0$. The conductivity of the inclusion is assumed to be one-tenth of the plate $\lambda = .1$. It is seen that as the size of the inclusion becomes larger the temperature at the inclusion interface increases and approach the constant values at the outer edges. In Fig. (2. 4) the inclusion size is held constant ($R/b = .5$) and the conductivity ratio λ is varied. Lowering the conductivity ratio increases the temperature at the interface to the case of an insulated circular hole, increasing the conductivity ratio λ approaches the case of the infinitely conducting inclusion which holds all of the heat. Figure 2. 5 displays the effect of plate size on the variation of normalized temperature ϕ for a given inclusion size $R/b = .5$ and a prescribed conductivity ratio $\lambda = .1$. It is seen that for $a/b = 4$ temperatures on the perimeter of the inclusion

are quite lower than the case of $\frac{a}{b} = .25$.

Figure 2.6 shows the normalized temperature distribution for a square plate with a circular inclusion determined by $\frac{R}{b} = .5$ and $\lambda = 10$. The curves represent the temperature variation for various values of $\gamma = \frac{y}{b}$. As $\frac{y}{b}$ increases the temperature approaches the linear distribution, thus verifying the fact that the effect of the inclusion dies out as the distance from the hole increases. The similar temperature distribution is presented in Fig. 2.7 for a lower conductivity ratio $\lambda = .1$. Again the temperature variation is almost linear for $\gamma = 1.0$ while the x-axis ($\gamma = 0$) shows the effect of the inclusion most. However due to the lower conductivity ratio, the temperature drop from the edge of the plate to the inclusion is less than in Fig. 2.6. Finally for square plate with a given inclusion size of $\frac{R}{b} = .75$, Fig. 2.8 shows the temperature distribution as a function of x, while the conductivity ratio is varied. Again the temperature differential from the plate edges $x = \pm a$ to the inclusion interface is less for the lower conductivity ratios.

III. THERMAL BENDING

In the second part of this study thermal bending problem of a rectangular elastic thin plate with an elastic inclusion by the least squares point matching method is investigated. The upper and lower surfaces of the plate are held at constant temperatures T_1' and T_2' respectively. (Fig. 3.1) The temperature is assumed to vary in the z-direction only. Hence

$$T = T(z) = T_o + \tau z \tag{3.1}$$

where

$$T_o = \frac{T_1' + T_2'}{2} \quad \text{with } T_1' > T_2' \text{ and } \tau = \frac{T_1' - T_2'}{2} \tag{3.2}$$

The governing equation for the transverse displacement w of a plate of uniform thickness t subjected to distributed transverse loading and nonuniform heating is [24]

$$D \nabla^2 \nabla^2 w = p(x, y) - \frac{1}{1-\nu} \nabla^2 M_T \tag{3.3}$$

where

$p(x, y)$ = Distributed transverse loading per unit area.

D = Bending rigidity of the plate per unit length $= E t^3/12(1-\nu^2)$

M_T = Thermal bending moment $= \alpha_t E \int_{-t/2}^{t/2} T(z)\, dz$

ν = Poisson's ratio

∇^2 = $\frac{\partial^2}{\partial x^2} + \frac{\partial^2}{\partial y^2}$

E = Young's modulus

α_t = Coefficient of thermal expansion

For the case of no transverse loading and a temperature distribution described by Eq. (3.1), the governing equation reduces to

$$\nabla^2 \nabla^2 w = 0 \tag{3.4}$$

The solution of equation (3.4) in plane polar coordinates can be represented as [25]

$$\begin{aligned} w = {} & A_o + B_o \ln r + C_o r^2 + D_o r^2 \ln r + [A_1 r\theta + B_1 r^{-1} + C_1 r^3 \\ & + D_1 r \ln r] \cos\theta + [A_1' r\theta + B_1' r^{-1} + C_1' r^3 + D_1' r \ln r] \sin\theta \\ & + D_o r^2 \theta + \sum_{m=2,3,\ldots}^{\infty} (A_m r^m + B_m r^{-m} + C_m r^{m+2} + D_m r^{-m+2}) \cos m\theta \\ & + \sum_{m=2,3,\ldots}^{\infty} (A_m' r^m + B_m' r^{-m} + C_m' r^{m+2} + D_m' r^{-m+2}) \sin m\theta \end{aligned} \tag{3.5}$$

By considering the symmetry of the problem two solutions, one, using the

subscript b, for the plate and one using the subscript a, for the inclusion are formulated from Eq. (3.5)

For the plate:

$$w_b = A_{ob} + B_{ob}\,\ell nr + C_{ob}\,r^2 + D_{ob}\,r^2\,\ell nr + \sum_{m=2,4,\ldots}^{\infty} (A_{mb}\,r^m + B_{mb}\,r^{-m} + C_{mb}\,r^{m+2} + D_{mb}\,r^{-m+2})\cos m\theta \tag{3.6}$$

For the inclusion:

$$w_a = A_{oa} + C_{oa}\,r^2 + D_{oa}\,r^2\,\ell nr + \sum_{m=2,4,\ldots}^{\infty} (A_{ma}r^m + C_{ma}r^{m+2})\cos m\theta \tag{3.7}$$

Here A_{oa}, A_{ob} to D_{oa}, D_{ob} and A_{ma}, A_{mb} to D_{ma}, D_{mb} represent the unknown coefficients to be determined from the boundary conditions. At the inclusion interface (r=R) there are four boundary conditions to contend with. They are

$$(M_r)_a = (M_r)_b;\ (Q_r^*)_a = (Q_r^*)_b$$
$$w_a = w_b;\ \frac{\partial w_a}{\partial r} = \frac{\partial w_b}{\partial r}. \tag{3.8}$$

where

$$M_r = \text{radial moment} = -D\left[\frac{\partial^2 w}{\partial r^2} + \nu\left(\frac{1}{r^2}\frac{\partial^2 w}{\partial \theta^2} + \frac{1}{r}\frac{\partial w}{\partial r}\right) + \frac{M_T}{(1-\nu)D}\right]$$

$$Q_r^* = \text{Kirchoff shear force} = Q_r + \frac{\partial M_{r\theta}}{\partial \theta}$$

Q_r = vertical shear force

$M_{r\theta}$ = twisting moment

Substituting Eqs. (3.6) and (3.7), into (3.8) one obtains the following four equations by combining the terms not under the summation sign.

$$D_a\left[2\,C_{oa}(1+\nu_a)+D_{oa}(3+2\,\ell n\,R)+D_{oa}\,\nu_a\,(1+2\,\ell n\,R)+\frac{M_{Ta}}{(1-\nu_a)D_a}\right]=D_b\left[\frac{B_{ob}}{R^2}(\nu_b-1)+2\,C_{ob}(1+\nu_b)+D_{ob}\,(3+2\,\ell n\,R)+D_{ob}\,\nu_b(1+2\,\ell n\,R)+\frac{M_T}{(1-\nu_b)D_b}\right] \tag{3.9}$$

$$D_a\,\frac{4D_{oa}}{R}=D_b\,\frac{4\,D_{ob}}{R} \tag{3.10}$$

$$A_{oa}+C_{oa}\,R^2+D_{oa}\,R^2\,\ell n\,R=A_{ob}+B_{ob}\,\ell n\,R+C_{ob}R^2+D_{ob}\,R^2\,\ell n R \tag{3.11}$$

$$2R\,C_{oa}+D_{oa}(R+2\,R\,\ell n\,R)=\frac{B_{ob}}{R}+2R\,C_{ob}+D_{ob}(R+2\,R\,\ell n\,R) \tag{3.12}$$

These four equations may be solved for A_{ob}, B_{ob}, C_{ob} and D_{ob}.

$$D_{ob}=\eta\,D_{oa}$$

$$B_{ob}=\alpha_1\,C_{oa}+\alpha_2\,D_{oa}+\alpha_3$$

$$C_{ob}=\alpha_4\,C_{oa}+\alpha_5\,D_{oa}+\alpha_6$$

$$A_{ob}=\alpha_7\,A_{oa}+\alpha_8\,C_{oa}+\alpha_9\,D_{oa}+\alpha_{10} \tag{3.13}$$

where

$$\begin{aligned}
\alpha_1 &= R^2[(1+\nu_b)-\eta(1+\nu_a)]\\
\alpha_2 &= \alpha_1[(1+2\,\ell nR)/2]\\
\alpha_3 &= -R^2/2\left[\frac{M_{Ta}}{(1-\nu_a)D_a}-\frac{M_{Tb}}{(1-\nu_b)D_b}\right]\\
\alpha_4 &= [\eta(1+\nu_a)+(1-\nu_b)]/2\\
\alpha_5 &= [(1+2\,\ell n\,R)/4]\,[(1-\nu_b)-\eta(1-\nu_a)]\\
\alpha_6 &= \alpha_3'-2\,R^2\\
\alpha_7 &= 1.0\\
\alpha_8 &= [R^2-\ell n\,R\,\alpha_1-R^2\,\alpha_4]\\
\alpha_9 &= [R^2\,\ell n\,R\,(1-\eta)-\ell n\,R\,\alpha_2-R^2\,\alpha_5]\\
\alpha_{10} &= -\ell n\,R\,\alpha_3-R^2\alpha_6
\end{aligned} \tag{3.14}$$

with

$$\eta = D_a/D_b$$

Combining the terms under the summation sign in the substitution of Eqs. (3.6) and (3.7) into (3.8) the following four equations in six unknowns are obtained

$$A_1 A_{ma} + A_2 C_{ma} = A_3 A_{mb} + A_4 B_{mb} + A_5 C_{mb} + A_6 D_{mb}$$

$$B_1 A_{ma} + B_2 C_{ma} = B_3 A_{mb} + B_4 B_{mb} + B_5 C_{mb} + B_6 D_{mb}$$

$$C_1 A_{ma} + C_2 C_{ma} = C_3 A_{mb} + C_4 B_{mb} + C_5 C_{mb} + C_6 D_{mb}$$

$$D_1 A_{ma} + D_2 C_{ma} = D_3 A_{mb} + D_4 B_{mb} + D_5 C_{mb} + D_6 D_{mb} \qquad (3.15)$$

Coefficients A_n, B_n, C_n, and D_n are given in the appendix B. One obtains the following expressions for C_{mb}, D_{mb}, B_{mb} and A_{mb} from these equations

$$C_{mb} = \beta_1 A_{ma} + \beta_2 C_{ma}$$

$$D_{mb} = \beta_3 A_{ma} + \beta_4 C_{ma}$$

$$B_{mb} = \beta_5 A_{ma} + \beta_6 C_{ma}$$

$$A_{mb} = \beta_7 A_{ma} + \beta_8 C_{ma} \qquad (3.16)$$

where

$$\beta_1 = 0, \quad \beta_2 = \frac{1-\nu_b + \eta(3+\nu_a)}{4}$$

$$\beta_3 = \frac{mR^{2m-2}}{4}\left[1-\nu_b - \eta(1-\nu_a)\right]$$

$$\beta_4 = \frac{R^{2m}(m+1)}{4}\left[(1-\nu_b) - \eta(1-\nu_a)\right]$$

$$\beta_5 = \frac{R^{2m}(1-m)}{4}\left[1-\nu_b - \eta(1-\nu_a)\right]$$

$$\beta_6 = \frac{R^{2m+2}}{m}\left[-1+\beta_2 + R^{-2m}(1-m)\,\beta_4\right]$$

$$\beta_7 = \frac{3+\nu_b - \eta(1-\nu_a)}{4}$$

$$\beta_8 = \frac{R^2(m+1)}{2m}\left[1+\nu_b - \eta(1+\nu_a)\right] \qquad (3.17)$$

Then Eq. (3.6) can be written as

$$w_b = \xi_1 A_{oa} + \xi_2 C_{oa} + \xi_3 D_{oa} + \xi_4 + \sum_{m=2,4,\ldots}^{\infty} (\xi_5 A_{ma} + \xi_6 C_{ma}) \cos m\theta \tag{3.18}$$

where:

$$\xi_1 = \alpha_7, \quad \xi_2 = \alpha_8 + \alpha_1 \ln r + \alpha_4 r^2$$

$$\xi_3 = \alpha_9 + \alpha_2 \ln r + \alpha_5 r^2 + \eta^2 \ln r$$

$$\xi_4 = \alpha_{10} + \alpha_3 \ln r + \alpha_6 r^2$$

$$\xi_5 = \beta_7 r^m + \beta_5 r^{-m} + \beta_1 r^{m+2} + \beta_3 r^{-m+2}$$

$$\xi_6 = \beta_8 r^m + \beta_6 r^{-m} + \beta_2 r^{m+2} + \beta_4 r^{-m+2} \tag{3.19}$$

The condition that the outer edges of the plate be simply supported requires that

at $x = \pm a$ and $y = \pm b$:

$$w_b = 0 \text{ and } M_n = -D_b \left(\frac{\partial^2 w_b}{\partial n^2} + \nu_b \frac{\partial^2 w_b}{\partial t^2}\right) - \frac{M_{Tb}}{1-\nu_b} = 0 \tag{3.20}$$

where n and t denote normal and tangential directions at the plate boundary respectively.

Substitution of Eq. (3.18) into the outer edge boundary conditions results in an infinite number of equations for the infinite number of unknown coefficients. As in the case of the first problem, the least squares boundary point matching method was employed. Namely the simply supported boundary conditions are satisfied at selected points, along the plate outer boundaries.

In order to present some numerical results, T_1' and T_2' are chosen as $150^\circ F$ and $100^\circ F$ respectively while the plate thickness is $\frac{a}{40}$. Forty points are taken along the outer boundaries of the plate (Fig. 2.2) and eight terms are considered in the series. Thus eighty equations in eleven unknowns are generated. Solving these in the least squares sense yields

the necessary coefficients.

In figures 3.2 and 3.3 the deflection function $\frac{w}{a^2}$ is presented as a function of $X = \frac{x}{a}$. The ratio of the inclusion rigidity to plate rigidity, $r = \frac{D_a}{D_b}$, is chosen as .1 and 10 respectively and the prescribed value of the ratio of the thermal moments $\rho = \frac{M_{Ta}}{M_{Tb}}$ =, is 1.0. Each figure presents the variation of the deflection function for three different inclusion sizes $\frac{R}{b}$ = .25, .50, and .75. In Fig. 3.2 the inclusion is less rigid than the plate and it is seen that the larger inclusion increases the plate deflection. However, in Fig. 3.3, the inclusion is more rigid than the plate and increasing the inclusion size decreases the plate deflection.

In Figs. (3.4) and (3.5) the deflection function is presented on the perimeter of the inclusion. The rigidity, thermal moment and Poisson ratio and inclusion size are held constant while the deflection at various radii is plotted. A comparison of these two figures indicates that the increase in the rigidity of the inclusion, causes lower deflection values at corresponding radii.

A summary of the effect of the inclusion rigidity is presented in Fig. 3.6. In this figure for a prescribed inclusion size the deflection function variation along the x-axis is shown as a function of the inclusion plate rigidity ratio r. The rigidity may be increased to the limit of the rigid inclusion where the deflection is constant across the inclusion surface, At the other extreme, the rigidity is lowered to the point where the inclusion gives no support and acts as a circular hole.

Finally in Fig. 3.7 the effect of the ratio of thermal moment ρ on the variation of the plate deflection is displayed. For a given inclusion size, constant elastic properties (E_a, E_b, ν_a and ν_b), the increase in the ratio

β which is directly related to the ratio of thermal expansion coefficients $\frac{\alpha_a}{\alpha_b}$, causes larger values in the deflection function.

APPENDIX A

THE LEAST SQUARE BOUNDARY POINT MATCHING METHOD

Given a linear function of the variables g_i defined by

$$f(x_k) = \sum_{i=1}^{N} a_i g_i(x_k) \tag{A-1}$$

where the g_i may be functions of any finite number of coordinates (x_k).

It is desired to determine the coefficients a_i such that $f(x_i)$ satisfies some specified conditions on some contour L. If L is not a coordinate line of the coordinate system in which the x_k are defined, it is presently impossible to do this exactly. However, if at some finite number $\bar{M}$ of points on L the specified conditions are satisfied, the following system of equations results.

$$F_m\left[f(x_k)\right] = F_m\left[\sum_{i=1}^{N} a_i g_i(x_k)\right] = b_m \tag{A-2}$$

where $(m = 1, \ldots, \bar{M})$. If F is a linear operator

$$b_m = \sum_{i=1}^{N} a_i F_m(g_i(x_k)) \qquad (m = 1, \ldots, \bar{M}) \tag{A-3}$$

Then if $\bar{M} = N$ the system is determined. However if $\bar{M} > N$ consider a solution to

$$\sum_{m=1}^{\bar{M}} \left[b_m - \sum_{i=1}^{N} a_i F_m(g_i(x_k))\right]^2 = d \tag{A-4}$$

where d is minimized with respect to the desired solution vector a_i.

That is

$$\min_{a_i} \sum_{m=1}^{\bar{M}} \left[b_m - \sum_{i=1}^{N} a_i F_m(g_i(x_k))\right]^2$$

It can be shown that if

$$a_i = \underset{\sim}{a}$$

$$F_m(g_i(x_k)) = [C]$$

and $b_m = \underset{\sim}{b}$ then for $\underset{\sim}{a}$ to minimize (A-2) for $\bar{M} > N$ it is necessary that $\underset{\sim}{a}$ be a solution of

$$[C]^T[C]\,\underset{\sim}{a} = [C]^T\,\underset{\sim}{b}$$

APPENDIX B

$$A_1 = [(m^2-m^3)(1-\nu_a)]\, R^{m-3}\eta$$

$$A_2 = [m^3(\nu_a-1) + m^2(3+\nu_a) + 4m]\, R^{m-1}\eta$$

$$A_3 = [(m^2-m^3)(1-\nu_b)]\, R^{m-3}$$

$$A_4 = [(m^2+m^3)(1-\nu_b)]\, R^{-m-3}$$

$$A_5 = [m^3(\nu_b-1) + m^2(3+\nu_b) + 4m]\, R^{m-1}$$

$$A_6 = [m^3(1-\nu_b) + m^2(3+\nu_b) - 4m]\, R^{-m-1}$$

$$B_1 = [(m^2-m)(1-\nu_a)]\, R^{m-2}\eta$$

$$B_2 = [m^2(1-\nu_a) + m(3+\nu_a) + 2(1+\nu_a)]\, R^{m}\eta$$

$$B_3 = [(1-\nu_b) \div (m^2-m)]\, R^{+m-2}$$

$$B_4 = [(1-\nu_b) \div (m^2+m)]\, R^{-m-2}$$

$$B_5 = [m^2(1-\nu_b) + m(3+\nu_b) + 2(1+\nu_b)]\, R^{m}$$

$$B_6 = [m^2(1-\nu_b) + m(-3-\nu_b) + 2(1+\nu_b)]\, R^{-m}$$

$$C_1 = R^{m}$$

$$C_2 = R^{m+2}$$

$$C_3 = R^{m}$$

$$C_4 = R^{-m}$$

$$C_5 = R^{m+2}$$

$$C_6 = R^{-m+2}$$

$$D_1 = mR^{m-1}$$

$$D_2 = (m+2)\, R^{m+1}$$

$$D_3 = mR^{m-1}$$

$$D_4 = -mR^{-m-1}$$

$$D_5 = (m+2)\,R^{m+1}$$

$$D_6 = (-m+2)\,R^{-m+1}$$

REFERENCES

1. Goodier, J. N. and Florence, A. L., Thermal stress due to disturbance of uniform heat flow by cavities and inclusions, Technical Report No. 120, Div. of Engr. Mech., Stanford University. (1959)

2. Florence, A. L. and Goodier, J. N., Thermal stress at spherical cavities and circular holes in uniform heat flow, J. Appl. Mech. 26, 293-294. (1959)

3. Florence, A. L., and Goodier, J. N., Thermal stresses due to disturbance of uniform heat flow by an insulated ovaloid hole, J. Appl. Mech. 27, 635-639. (1960)

4. Goodier, J. N. and Florence, A. L., Thermal stresses at an insulated circulated hole near the edge of an insulated plate under uniform heat flow, Quart. J. Mech. Appl. Math. 16, 273-282. (1963)

5. Florence, A. L. and Goodier, J. N., Thermal stress due to disturbance of uniform heat flow by an insulated spheroidal cavity, Proc. 4th U. S. National Cong. Appl. Mech. pp. 595-602. (1962)

6. Goodier, J. N. and Florence, A. L., Localized thermal stress at holes, cavities and inclusions disturbing uniform heat flow, thermal crack propagation, Proc. Eleventh Intern. Cong. Appl. Mech. (1964)

7. Goland, M., The Influence of the shape and rigidity of an elastic inclusion on the transverse flexure of thin plates, J. of Appl. Mech., pp. 69-75. (1943)

8. Tauchert, T. R., Thermal stresses at spherical inclusions in uniform heat flow, J. Composite Materials, vol. 2, no. 4, pp. 478-486. (1968)

9. Hoffman, R. E. and Ariman, T., Thermal bending of plates with circular holes, Nuclear Eng. Design, vol. 14, pp. 231-238, (1970)

10. Rao, K. S., Rao, M. N. and Ariman, T., Thermal stresses in plates with circular holes, Nuclear Eng. Design, vol. 15, pp. 97-112. (1971)

11. Rao, K. S., Rao, M. N. and Ariman, T., "Thermal stresses in plates with circular holes, Nuclear Eng. Design, vol. 15, pp. 97-112. (1971)

12. Slater, J. C., Electron energy bands in metals, Physical Review, vol. 45, pp. 794-801. (1934)

13. Barta, J., On the numerical solution of a two -dimensional elasticity problem, Zietschrift fur Angewandte Mathematik und Mechanik, vol. 7, no. 3, pp. 184-185. (1937)

14. Conway, H. D., The approximate analysis of certain boundary value problems, J. of Applied Mech., vol. 27, pp. 275-277. (1960)

15. Leissa, A. W. and Niedenfuhr, F. W., A study of the Cantilevered square plate subjected to a uniform loading, J. of the Aero/Space Sc., pp. 162-169. (1962)

16. Leissa, A. W. and Niedenfuhr, F. W., Bending of a square plate having two adjacent edges free and the other clamped or simply supported, J. of the Amer. Inst. of Aeronautics and Astronautics, pp. 116-120. (1963)

17. Neidenfuhr, F. W., Leissa, A. W., and Lo, C. C., A study of the point-matching method as applied to thermally and transversely loaded plates and other boundary value problems, Technical Report No. AFFDL-TR-64-159, (1964)

18. Niedenfuhr, F. W., Leissa, A. W. and Lo, C. C., Further studies in the application of the point-matching technique to plate bending and other harmonic and biharmonic boundary value problems, Technical Report No. AFFDL-TR-65-114. (1965)

19. Lo, C. C., and Leissa, A. W., Bending of plates with circular holes, Acta Mech., vol. 1, pp. 64-74. (1967)

20. Eringen, A. C., Naghdi, A. K. and Thiel, C. C., State of stress in a circular cylindrical shell with a circular hole, Welding Research Council Bulletin No. 102. (1965)

21. Eringen, A. C., Naghdi, A. K., Mahmood, S. S., Thiel, C. C. and Ariman, T., Analysis of stress and deformation in two normally intersecting cylindrical shells subject to internal pressure, Gen. Tech. Rep. No. 3-8. (1965)

22. Eringen, A. C., Naghdi, A. K., Mahmood, S. S., Thiel, C. C. and Ariman, T., Stress concentrations in two normally intersecting cylindrical shells subject to internal pressure, Welding Research Council Bulletin No. 139 (1969)

23. Carslaw, H. S. and Jaeger, J. C., Conduction of heat in solids, Oxford Press (1959)

24. Boley, B. A. and Weiner, J. H., Theory of thermal stresses, John Wiley and Sons, pp. 378-388. (1960)

25. Mitchell, J. H., Proc. London Math. Soc., 31, 100, (1899)

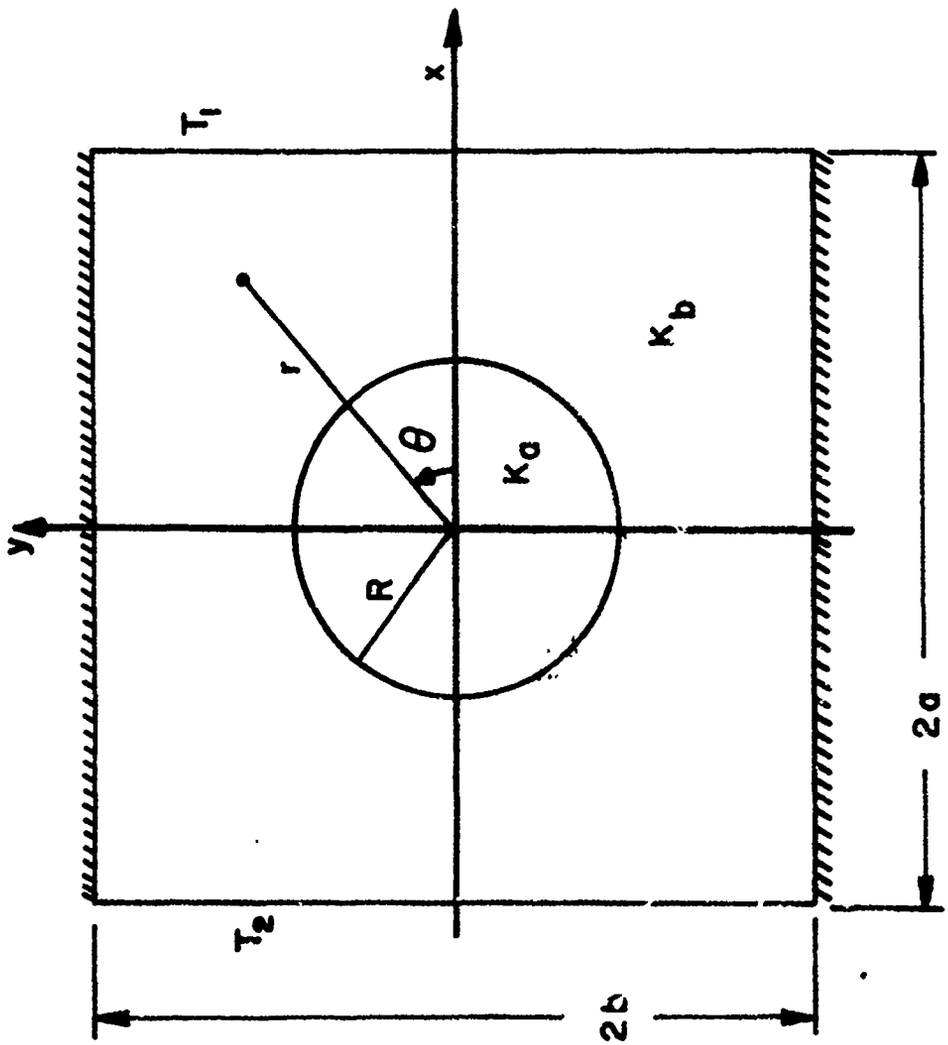

Fig. 2.1 - System of co-ordinates for temperature distribution.

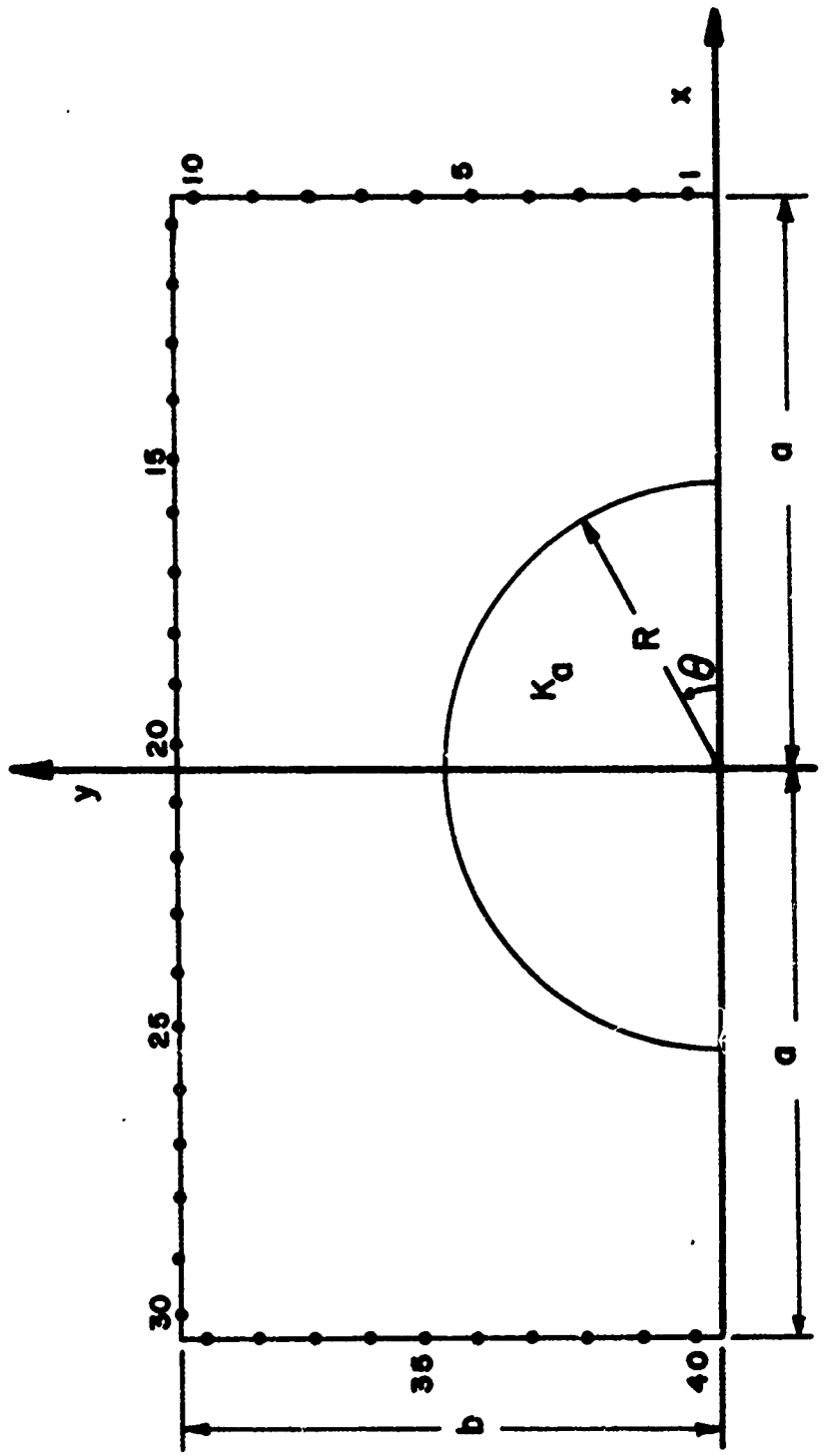

Fig. 2.2 Typical boundary layout for "point-matching".

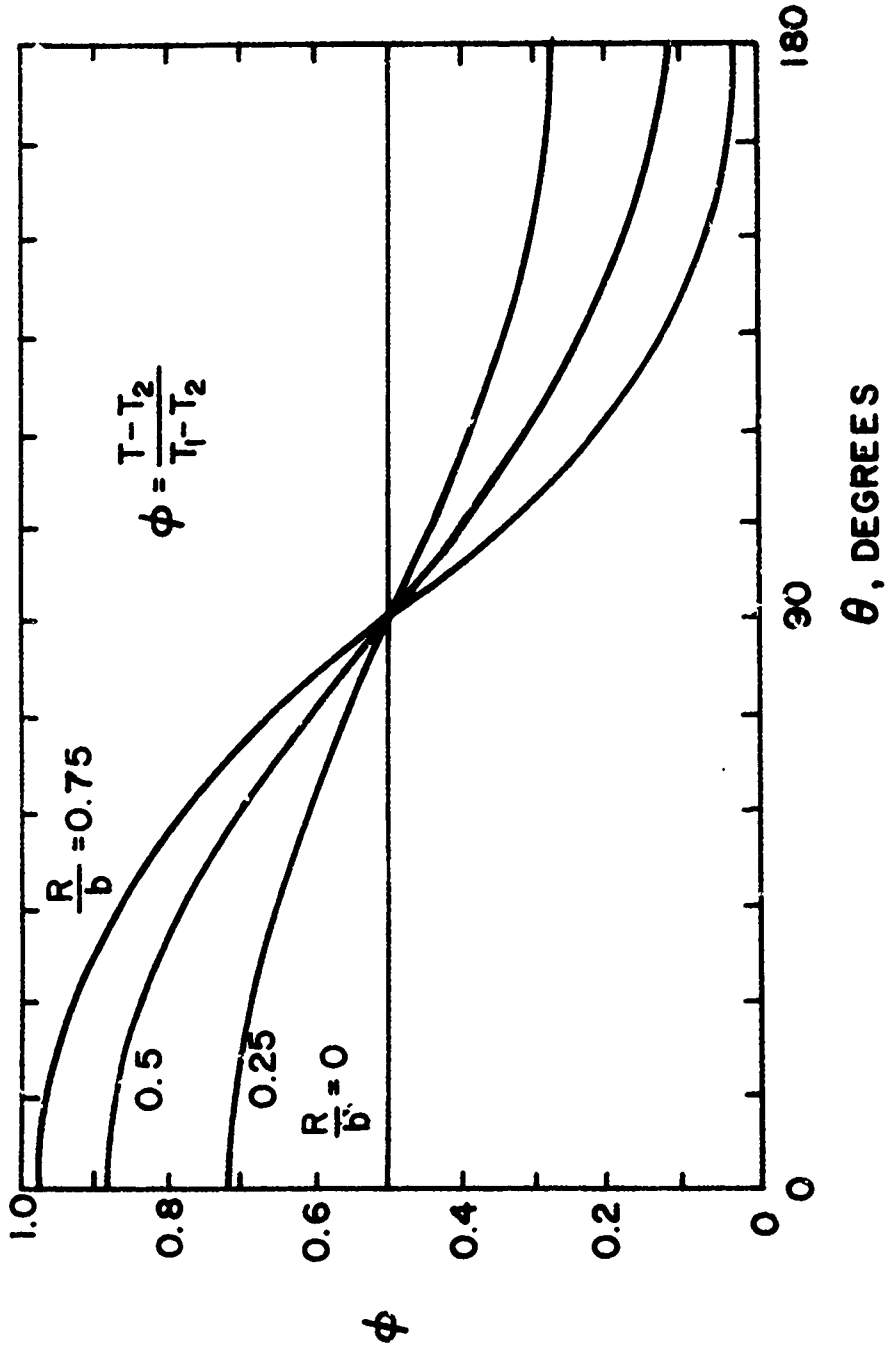

Fig. 2.3 Temperature function ϕ, plotted as a function of inclusion size and θ for $\lambda = .1$, $\frac{a}{b} = 1.0$, and $r = R$.

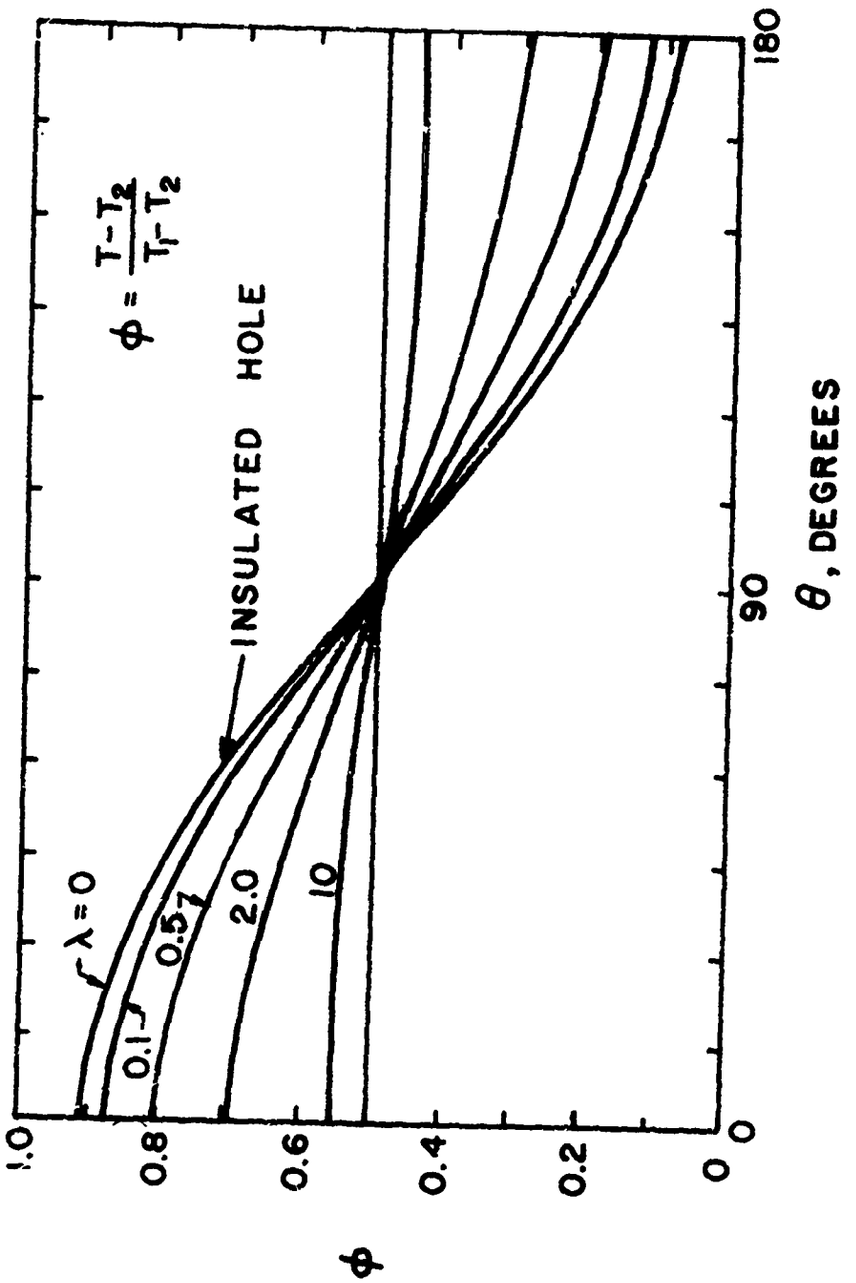

Fig. 2.4 Temperature function φ, plotted as a function of λ and θ for R/b = .5, a/b = 1.0, and r = R.

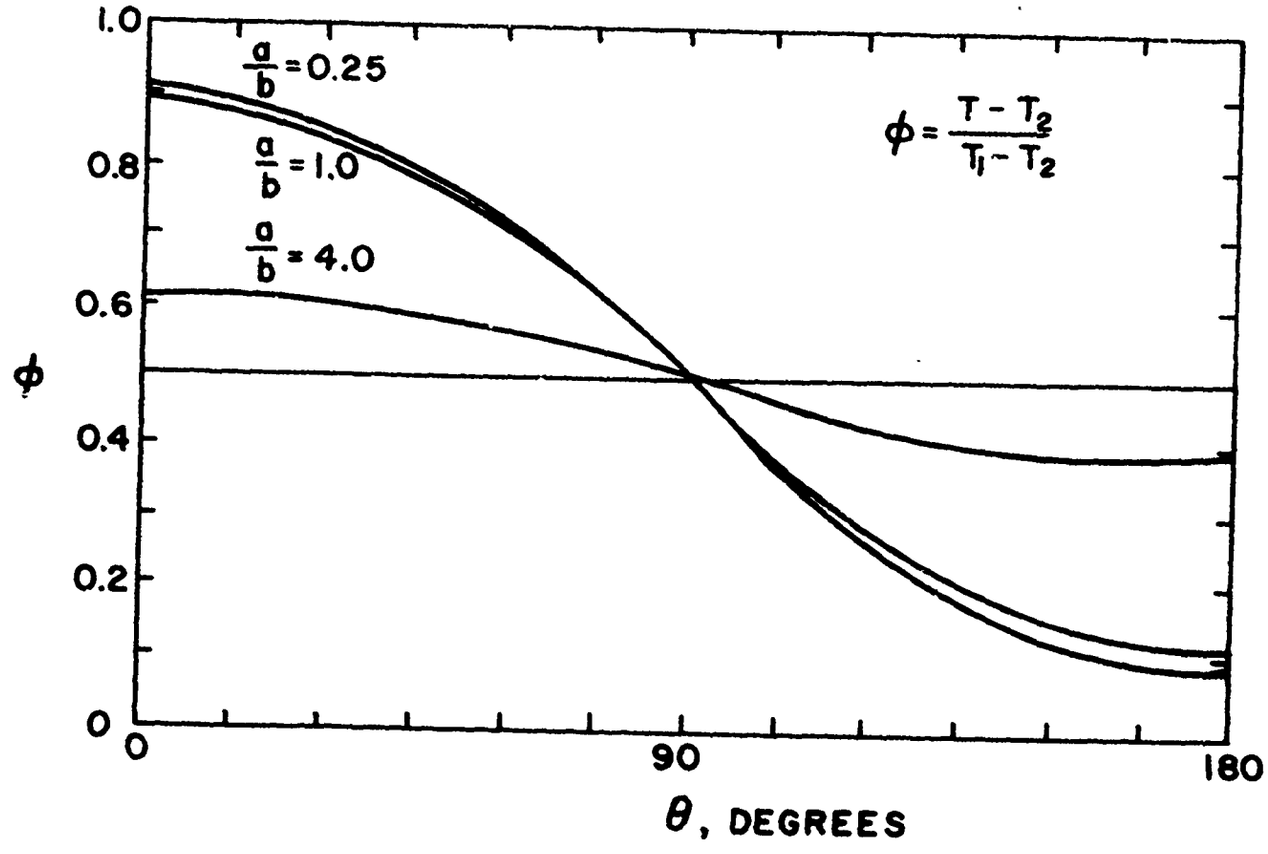

Fig. 2.5 Temperature function φ, plotted as a function of a/b and θ, with R/b = .5 and λ = .1, and r = R.

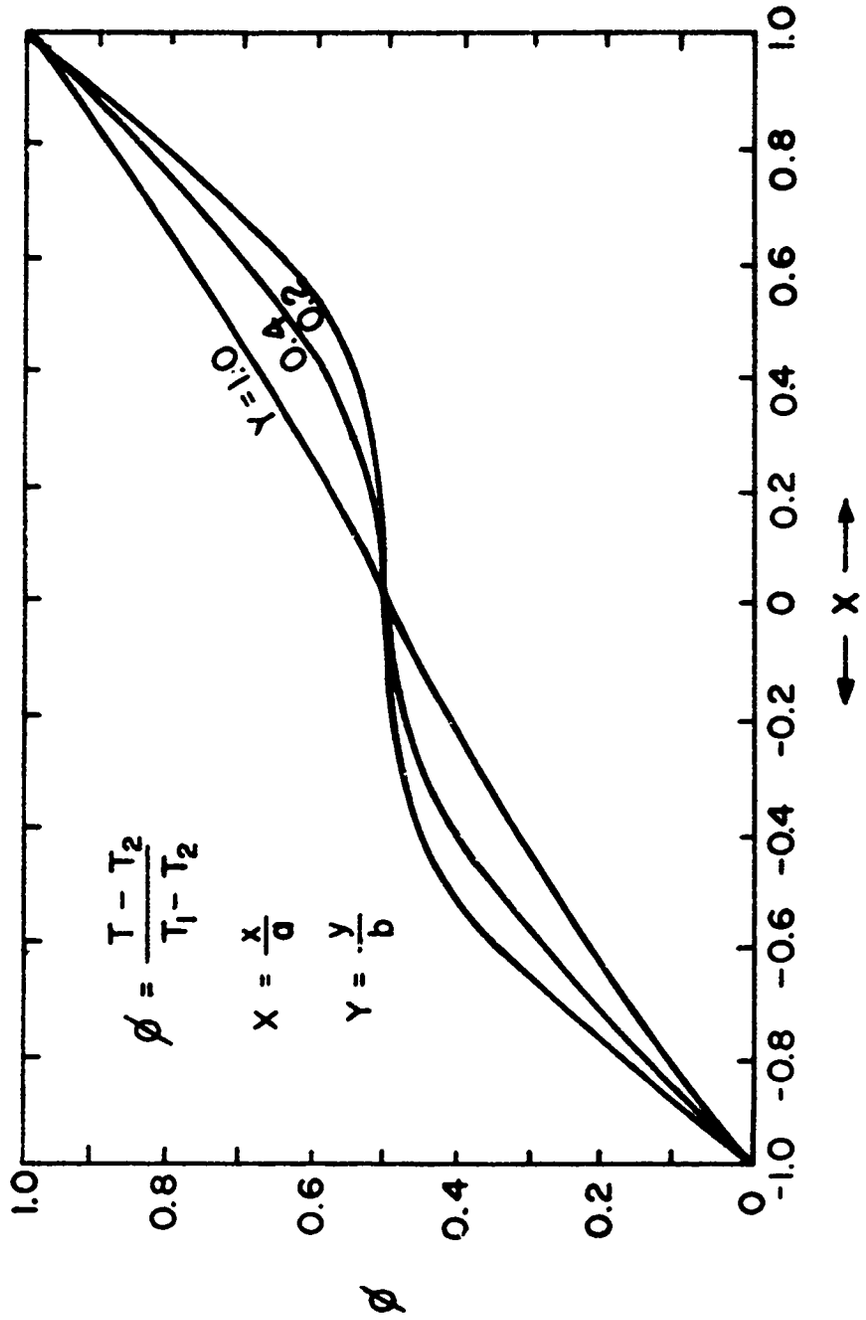

Fig. 2.6 Temperature function ϕ, plotted as a function of X and Y with $R/b = .5$, $a/b = 1.0$, $\lambda = 10$.

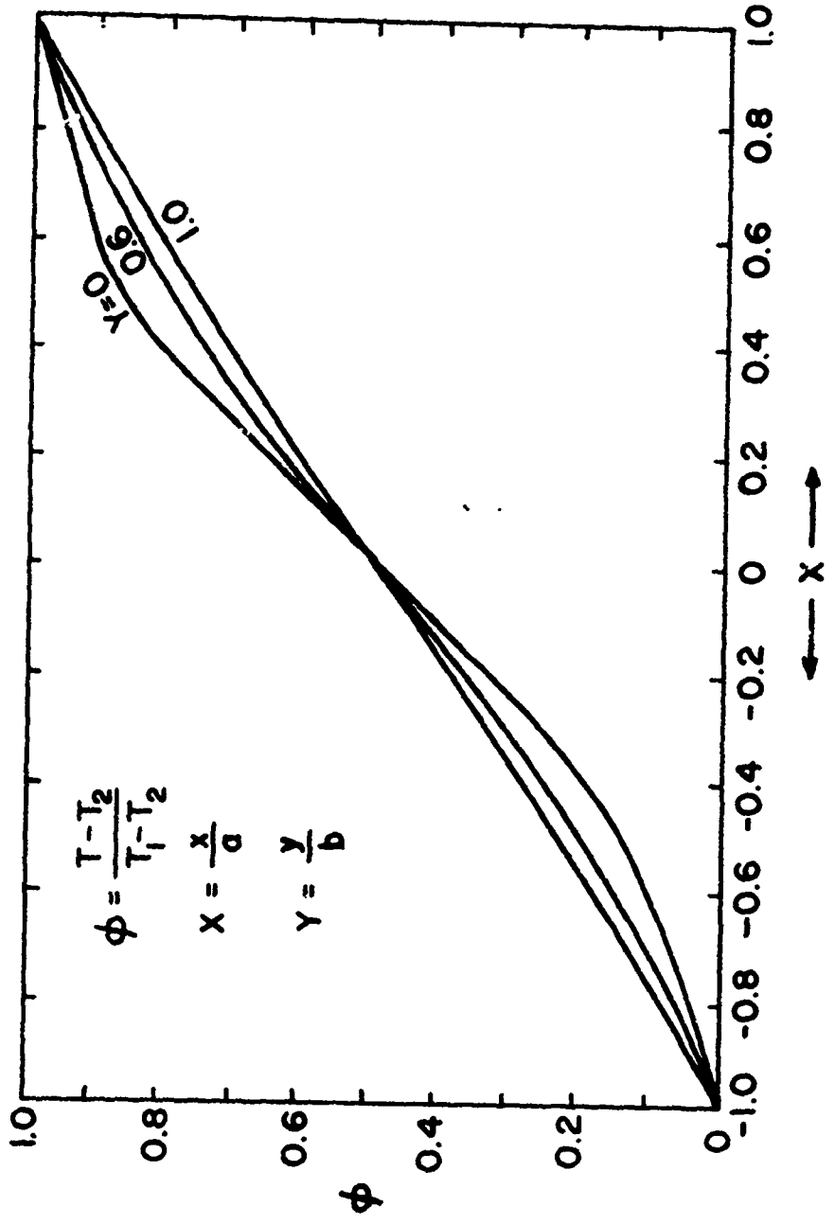

Fig. 2.7 Temperature function ϕ, plotted as a function of X and Y with $R/b = .5$, $a/b = 1.0$, $\lambda = .1$.

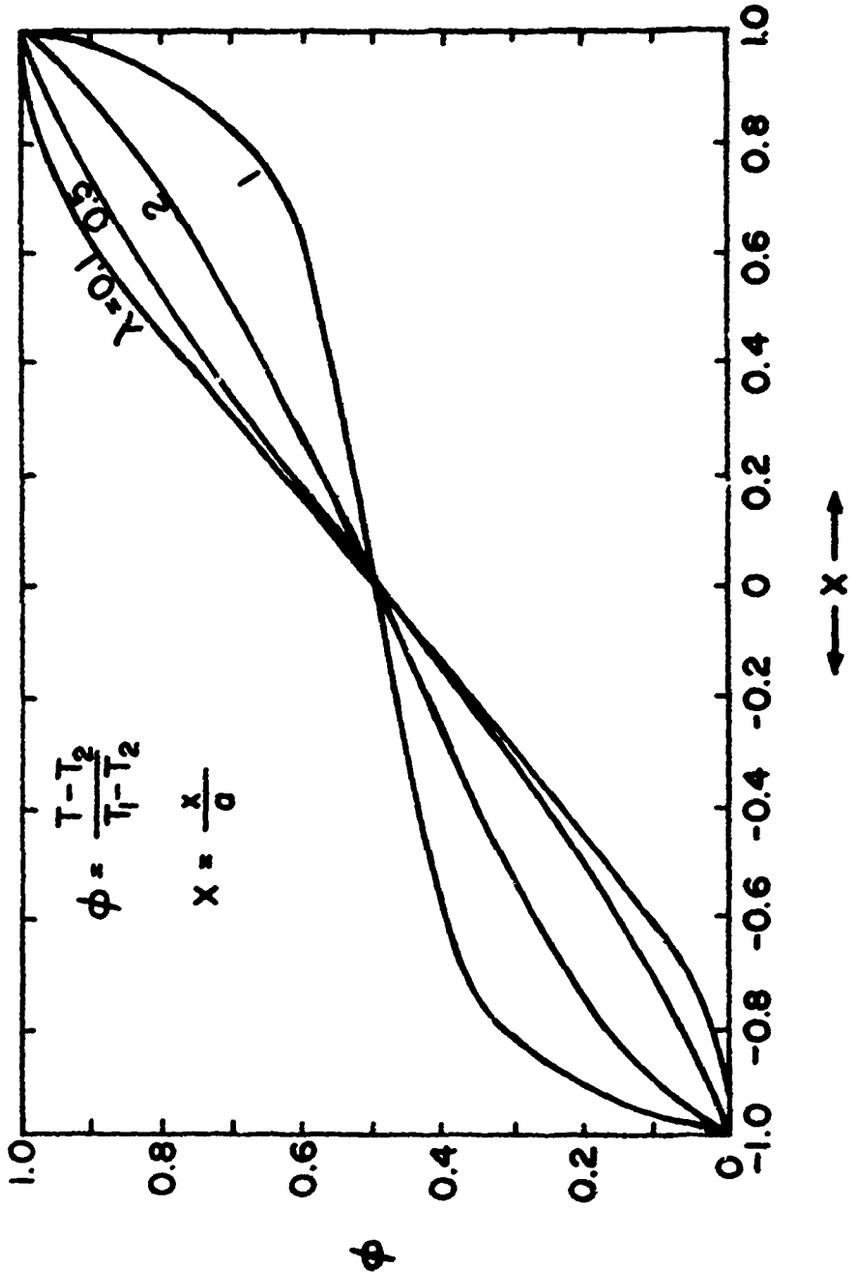

Fig. 2.8 Temperature function ϕ, plotted as a function of X and λ with $R/b = .75$, $a/b = 1.0$, $y = 0.0$.

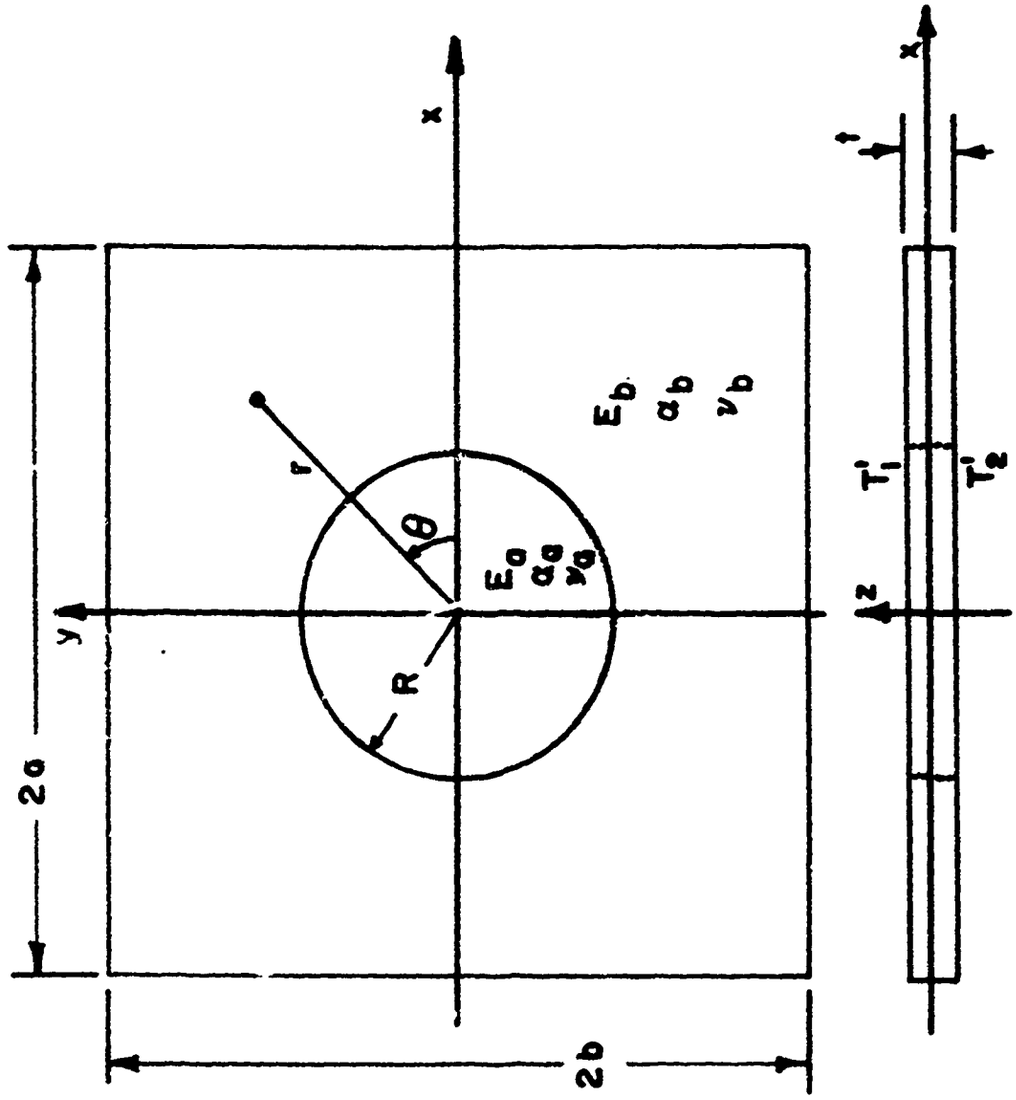

Fig. 3.1 Simply supported rectangular plate with circular inclusion - coordinate system.

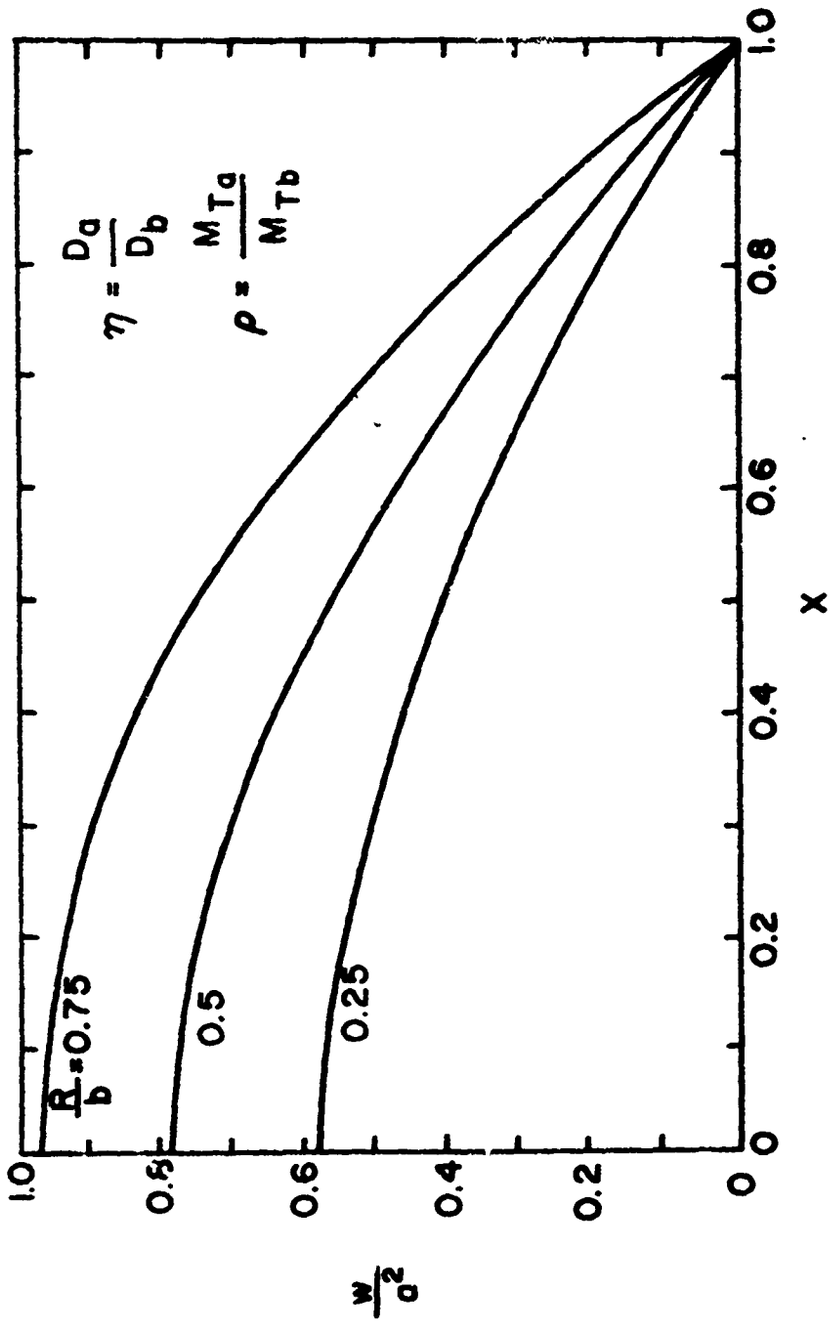

Fig. 3.2 Plate deflection as a function of R/b with $\eta = .1$, $\rho = 1.0$, and $\nu_a = \nu_b = .3$.

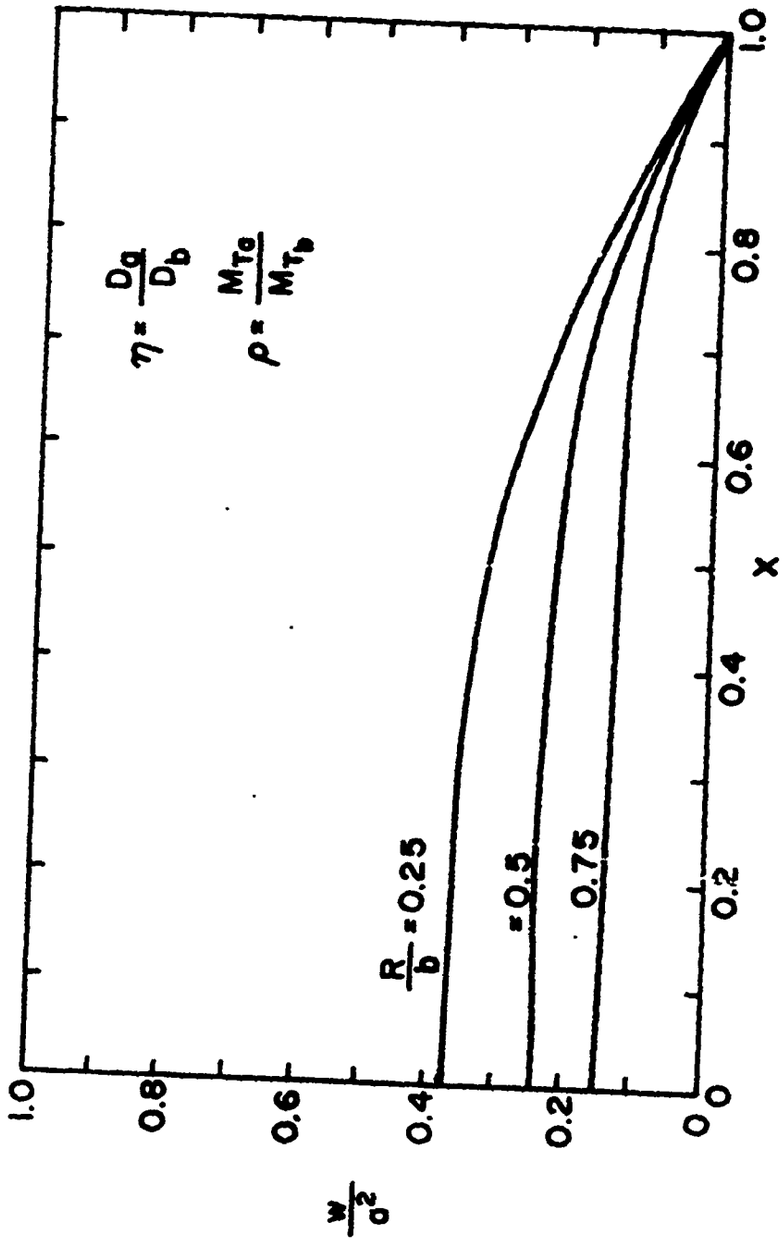

Fig. 3.3 Plate deflection as a function of R/b with $\eta = 10.0$, $\rho = 1.0$ and $\nu_a = \nu_b = .3$.

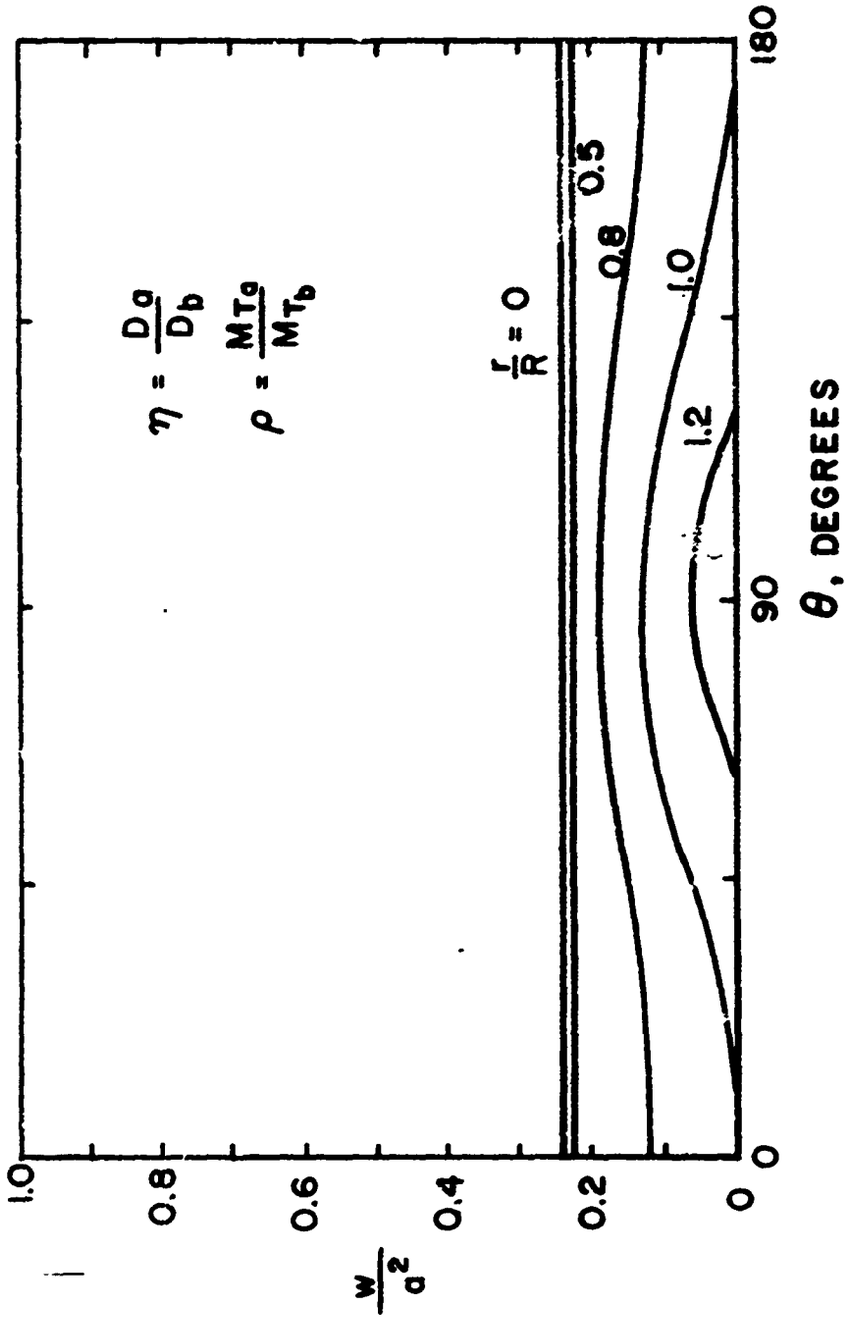

Fig. 3.4 Plate deflection as a function of θ with η =1.0, ρ = 1.0, R/b = .5 and $\nu_a = \nu_b$ = .3 .

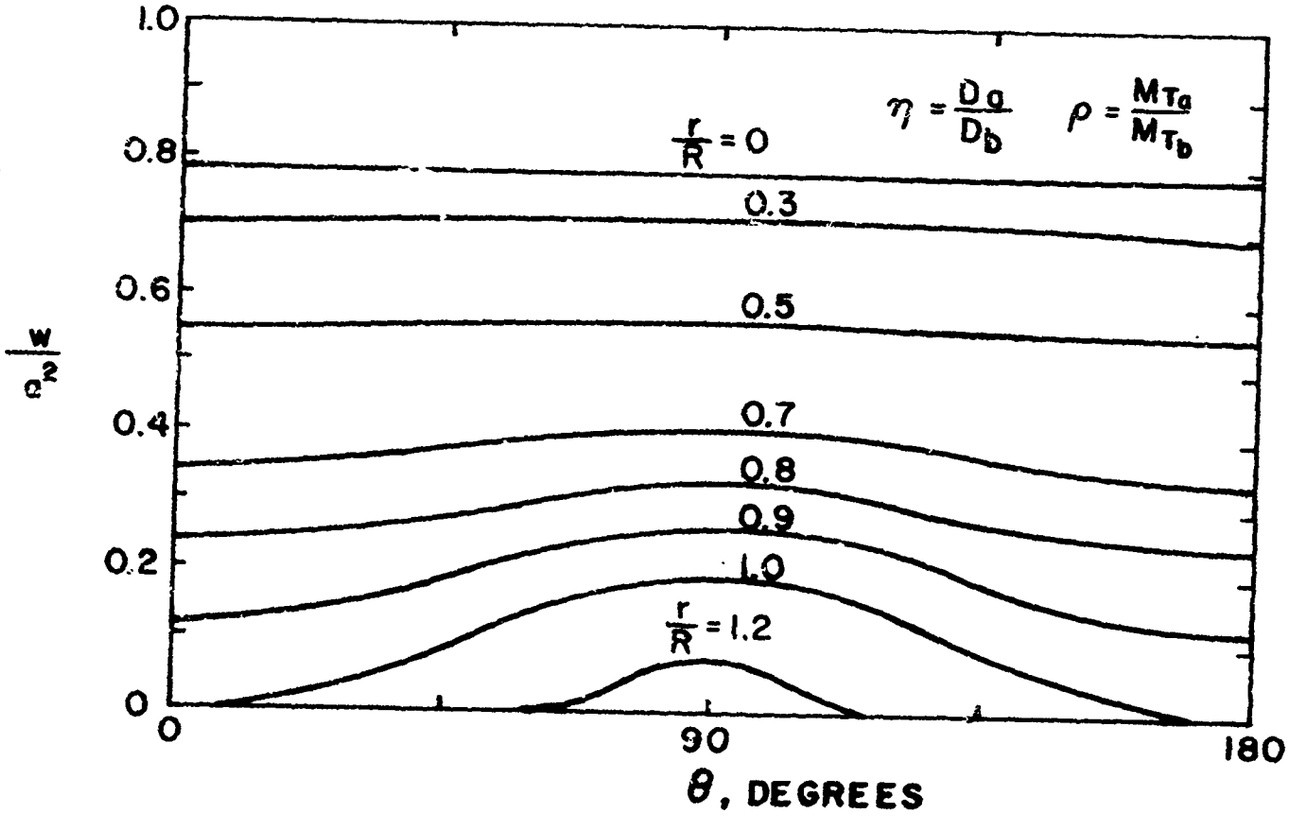

Fig. 3.5 Plate deflection as a function of θ with $\eta = .1$, $\rho = 1.0$, $R/b = .5$ and $\nu_a = \nu_b = .3$.

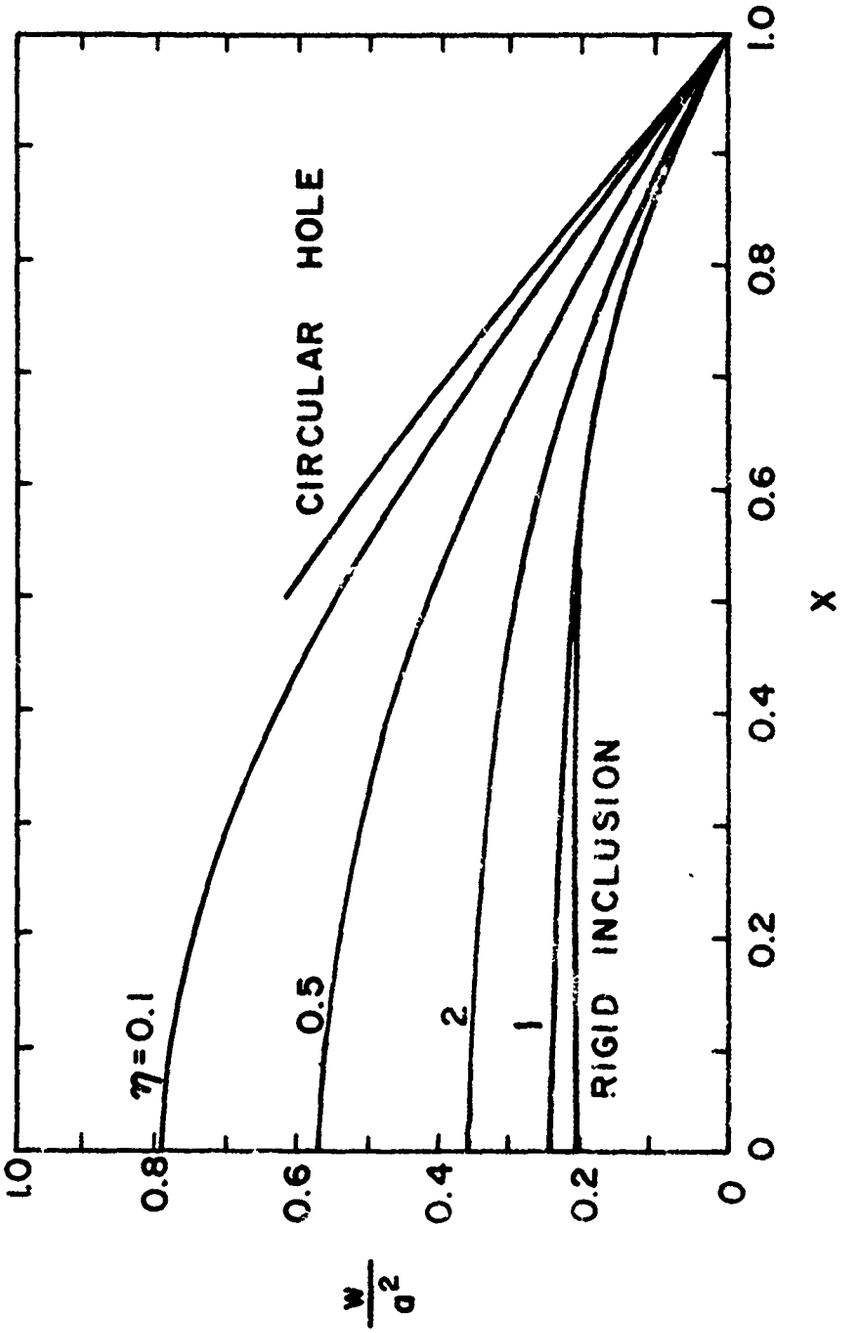

Fig. 3.6 Plate deflection as a function of η with $R/b = .5$, $\rho = 1.0$ and $\nu_a = \nu_b = .3$.

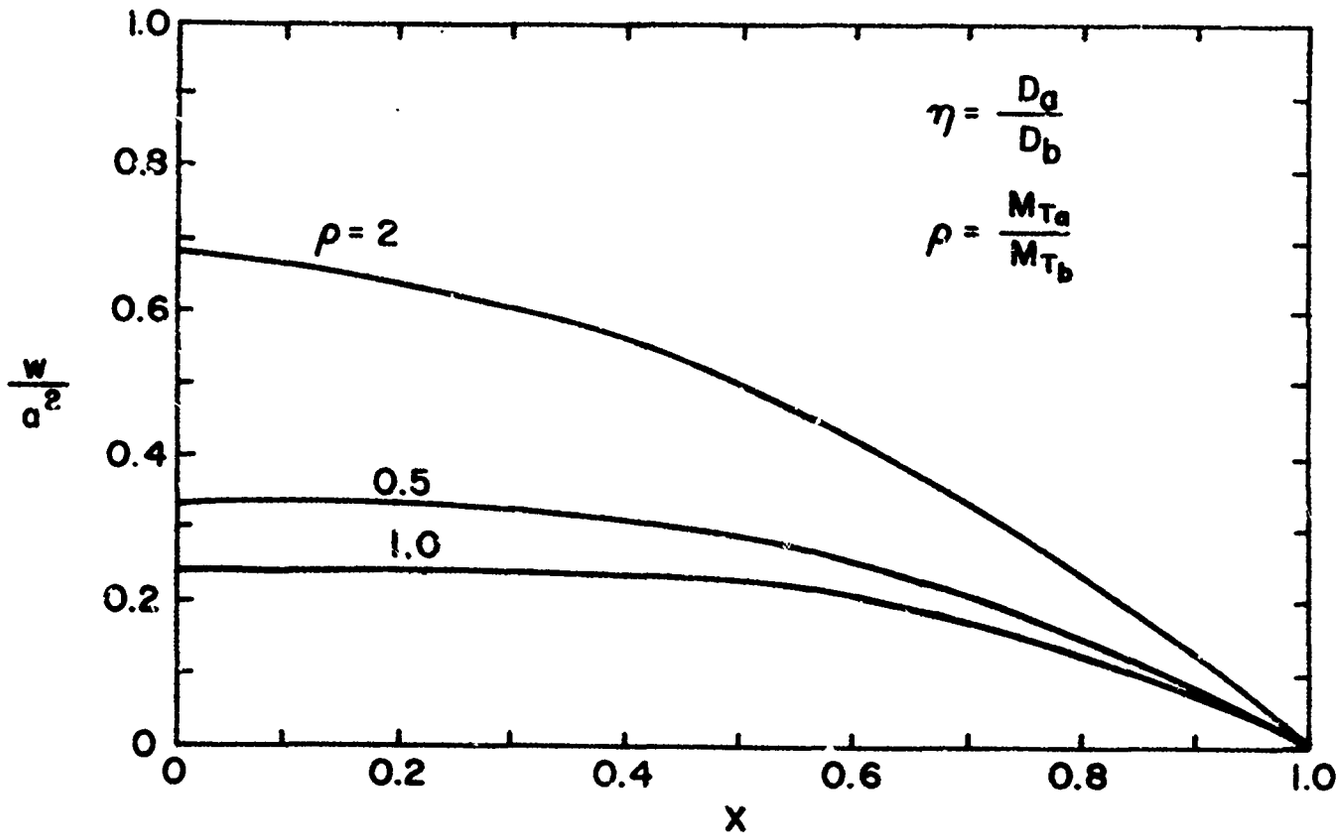

Fig. 3.7 Plate deflection as a function of ρ with $\eta = 1.0$, $R/b = .15$, $\nu_a = \nu_b = .3$.